6-24-2016

Effects of Electrode Off Centre on Trapped Thickness-Shear Modes in Contoured AT-Cut Quartz Resonators

Junjie Shi
Zhengzhou University

Cuiying Fan
Zhengzhou University

Minghao Zhao
Zhengzhou University

Jiashi S. Yang
University of Nebraska- Lincoln, jyang1@unl.edu

Effects of Electrode Off Centre on Trapped Thickness-Shear Modes in Contoured AT-Cut Quartz Resonators

Junjie Shi

Department of Aeronautical Mechanical Engineering, Aviation Maintenance NCO Academy of Air Force Engineering University, Xinyang 464000, China.
School of Chemical Engineering and Energy, Zhengzhou University, 100 Science Road, Zhengzhou 450001, China.

Cuiying Fan and Minghao Zhao

School of Mechanical Engineering, Zhengzhou University, 100 Science Road, Zhengzhou 450001, China.

Jiashi Yang

School of Chemical Engineering and Energy, Zhengzhou University, 100 Science Road, Zhengzhou 450001, China.
Department of Mechanical and Materials Engineering, University of Nebraska-Lincoln, W340 Nebraska Hall, 820 N 16th St., Lincoln, NE 68588-0526, USA.

(Received 20 May 2015; accepted 24 June 2016)

We investigated thickness-shear vibrations of a contoured, AT-cut quartz resonator with a pair of electrodes displaced from the resonator centre. The scalar differential equations by Stevens and Tiersten for thickness-shear vibrations of electroded and unelectroded quartz plates were employed. Based on the variational formulation of the scalar differential equations established in a previous paper and the variation-based Ritz method with trigonometric functions as basis functions, free vibration resonance frequencies and trapped thickness-shear modes were obtained. The effects of the electrode off centre on resonance frequencies and mode shapes were examined. When the electrode off centre is about one hundredth of the electrode length, the relative frequency shift is of the order of one part per million, significant in certain resonator design and applications. The electrode off centre also causes the loss of symmetry of modes, which has an adverse effect on resonator frequency stability under a normal acceleration.

1. INTRODUCTION

Piezoelectric crystal resonators are widely used as frequency standards for time-keeping and frequency operation with broad applications in telecommunication and sensing. They have been under sustained study experimentally, numerically, and theoretically.[1–13] Most crystal resonators operate with thickness-shear (TSh) modes of quartz plates. Contoured plate resonators with nonuniform thickness are used for strong energy trapping of their operating TSh modes, in which the TSh vibration is confined near the resonator centre and decays toward the resonator edge. Metal electrodes on crystal resonators are necessary for electrically exciting acoustical vibrations through piezoelectric coupling. In a typical quartz plate resonator, there are two electrodes on the plate's top and bottom surfaces. They cover the central part of the plate surfaces only, leaving the border part of the plate unelectroded. Ideally, the two electrodes should be identical and are perfectly placed at the centre of the resonator. However, in real resonator manufacturing, one electrode is pre-deposited with a predetermined thickness. Then the electrode on the other side of the plate has a thickness that is determined by the frequency of the electroded plate. This usually results in a plate with two electrodes of slightly different thicknesses. In addition, the location of the centre of the electrodes may be slightly off the centre of the crystal plate due to manufacturing imperfections.

Since the frequency requirement of crystal resonators is very high (usually in terms of parts per million or *ppm* for civilian applications and several orders of magnitude higher in military applications), the effects of imperfect electrodes have been a constant concern in resonator design and manufacturing. The effects of electrodes of unequal thicknesses can be taken into consideration into a theoretical analysis in a relatively simple manner and has been studied by many researchers.[14–17] It has been shown that, for frequency consideration, to the lowest order, it is the total thickness of the two electrodes that matters. However, for the effects of off-centre electrodes, the problem is much more complicated and challenging. Theoretical results on off-centre electrodes are very few. The only relevant reference known to the authors of the present paper is He et al.,[18] which is on a related but different problem of mismatched or unequal electrodes. The analysis in He et al.[18] was

for the relatively simple case of a flat resonator in the special case of straight crested modes with the TSh displacement varying along one of the two in-plane directions of the plate, x_3, only. In addition to the frequency effect, it is also known that off-centre electrodes can cause symmetry loss in TSh modes which has important implications in resonator frequency stability.[19,20] In general, the effects of off-centre electrodes are still mostly unknown. They are potentially important and need to be quantified.

In this paper, we study the effects of off-centre electrodes in a contoured resonator with modes varying along both of the in-plane directions of the plate, x_3 and x_1. Both the effects on frequency and on mode shapes are considered.

2. CONTOURED RESONATOR WITH OFF-CENTRE ELECTRODES

Consider a partially electroded, contoured quartz plate resonator of a variable thickness $2h$ with electrode off centre as sketched in Fig. 1. In this paper we study the case where the top and bottom electrodes shift in the same way. The case where the two electrodes shift differently is important in applications but it cannot be modelled within the theoretical framework of the present paper and remains challenging.

Specifically, the thickness of the resonator is varying according to:[21]

$$2h = 2h_0[1 - \frac{({x_1}^2 + {x_3}^2)}{4Rh_0}]; \tag{1}$$

where R is the radius of curvature of the spherical surface of the contoured resonator and $2h_0$ is the centre thickness. $2l$ is the electrode length. $2h'$ is the electrode thickness. We note that for large $({x_1}^2 + {x_3}^3)^{\frac{1}{2}}$ Eq. (1) may result in a zero or even negative thickness. This is not a problem because, as the results will show, in contoured resonators, the vibration dies out quickly away from the centre of the plate before the plate thickness diminishes to zero. Therefore it does not matter what the plate thickness is for large $({x_1}^2 + {x_3}^3)^{\frac{1}{2}}$. The active region of the resonator is characterized by a small $({x_1}^2 + {x_3}^3)^{\frac{1}{2}}$. For small $({x_1}^2 + {x_3}^3)^{\frac{1}{2}}$ we have, approximately:[21]

$$\frac{1}{(2h)^2} \cong \frac{1}{(2h_0)^2}[1 + \frac{({x_1}^2 + {x_3}^2)}{2Rh_0}]. \tag{2}$$

3. VARIATIONAL ANALYSIS

The TSh motion of the resonator in Fig. 1 is governed by the scalar differential equations[22–26] which take slightly different forms for the electroeded and unelectroded parts of the resonator. In our previous paper,[27] the scalar equations were written in variational form which provides the theoretical foundation for analysing quartz TSh resonators using variation-based techniques. The variational formulation has been shown to be effective in the analyses of a flat resonator[27] and a contoured resonator,[28] and both were perfect resonators without electrode

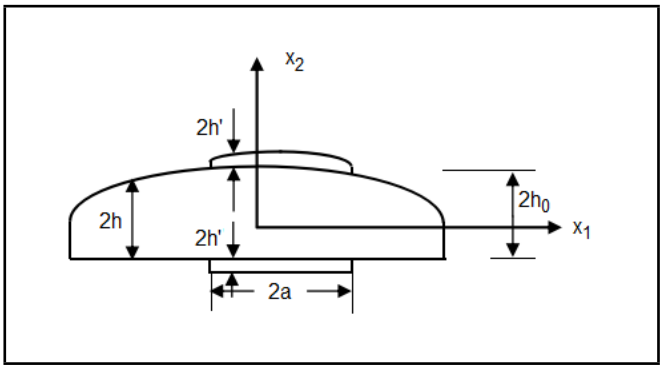

Figure 1. Side view of a contoured resonator with its varying thickness and electrode off centre.

off centre. Below, we use the Ritz method based on the variational formulation to analyse the free vibration of the contoured resonator in Fig. 1 with electrode off centre.

The procedure and the major equations of the variational formulation are formally the same as those in Shi et al.[27] and therefore are not repeated here. However, since the resonator in the present paper is contoured and is with electrode off centre, there are significant complications. One is that the ${\overline{\omega}_n}^2$ and ${\omega_n}^2$ in Eq. (7)[27] are no longer constants and are functions of x_1 and x_3 as follows through Eq. (2):[28]

$$\begin{aligned} {\overline{\omega}_n}^2 &\cong \frac{n^2\pi^2\hat{c}^{(1)}}{\rho 4{h_0}^2}[1 + \frac{({x_1}^2 + {x_3}^2)}{2Rh_0}]; \\ {\omega_n}^2 &\cong \frac{n^2\pi^2\bar{c}^{(1)}}{\rho 4{h_0}^2}[1 + \frac{({x_1}^2 + {x_3}^2)}{2Rh_0}]. \end{aligned} \tag{3}$$

Eq. (3) already appeared[28] for a contoured resonator without electrode off centre. The major complication in the present paper is that because of the electrode off centre and the related symmetry loss of the resonator structure, the basis functions of the Ritz method[27,28] need to be extended greatly. To be specific, consider the rectangular resonator with electrode off centre in Fig. 2. According to the Ritz method, we construct the following expression for the TSh displacement field using the modes of a rectangular plate with a uniform thickness as basis functions[25]:

$$\begin{aligned} {u_1}^n = &\sum_{m,p} A_{mp} cos(\frac{m\pi x_1}{2l}) cos(\frac{p\pi x_3}{2w}) + \\ &+ \sum_{m_1,p_1} A_{m_1p_1} sin(\frac{m_1\pi x_1}{2l}) cos(\frac{p_1\pi x_3}{2w}) + \\ &+ \sum_{m_2,p_2} A_{m_2p_2} cos(\frac{m_2\pi x_1}{2l}) sin(\frac{p_2\pi x_3}{2w}) + \\ &+ \sum_{m_3,p_3} A_{m_3p_3} sin(\frac{m_3\pi x_1}{2l}) sin(\frac{p_3\pi x_3}{2w}); \end{aligned} \tag{4}$$

where A_{mp}, $A_{m_1p_1}$, $A_{m_2p_2}$ and $A_{m_3p_3}$ are undetermined constants. The series expansion of the TSh displacement in Eq. (4) has to include basis functions symmetric and antisymmetric in both x_3 and x_1. As a consequence Eq. (4) is four times as long as the series expansion[27,28] when there was no electrode off

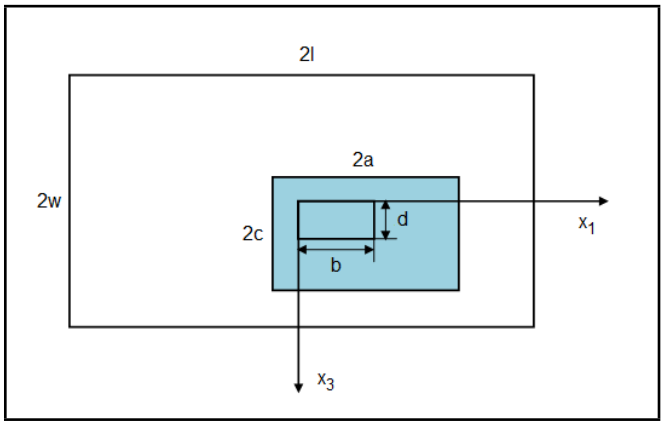

Figure 2. A rectangular resonator with electrode off centre.

centre. Eq. (4) is substituted into the variational functional,[27] resulting in a quadratic form of the undetermined constants. The minimization of the quadratic form leads to a system of linear homogeneous equations for the undetermined constants. For nontrivial solutions of the undetermined constants, the determinant of the coefficient matrix of the linear equations has to vanish, which yields the frequency equation. For each frequency, the corresponding nontrivial solution of the undetermined constants from the homogeneous equations determines the corresponding mode shape. These are very complicated and are carried out on a computer.

4. NUMERICAL RESULTS AND DISCUSSION

Consider an AT-cut quartz resonator with a typical centre thickness $2h_0 = 0.68783\ mm$, radius of curvature of the contour $R = 2000\ mm$, electrode/plate mass ratio $R' = 1.869 \times 10^{-3}$, square electrodes of $a = c = 5\ mm$, and square plate with $l = w = 3a$. For the modes of interest with slow in-plane variations along x_3 and x_1, numerical tests show that the trigonometric series in Eq. (4) converges rapidly. When 10 or 11 terms are kept in each of the x_1 and x_3 directions, the fundamental TSh frequency found has seven significant figures. This is sufficient for ordinary resonator design. Ten terms in each direction are used for the rest of the numerical calculation. Generally, contoured resonators are used on the overtones, e.g., $n = 3$ or $n = 5$. Our theoretical formulation is valid for any n. In the following we consider the fundamental mode with $n = 1$ for numerical examples. It is known that modes with larger values of n are qualitatively similar but decay faster outside the electroded region. The numerical results are organized in the following order. The case of a perfect resonator without electrode off centre is presented first as a reference. Then we examine three separate cases with electrode off centre. We vary d alone first with b fixed. Then we vary b alone with d fixed. Finally we vary both d and b simultaneously.

Fig. 3 shows the operating mode of the resonator in the case of $b = 0$ and $d = 0$, i.e., the case without electrode off centre as a reference. Both a three-dimensional view and a contour view of the distribution of the TSh displacement in the plane of the plate are given. The mode is perfectly symmetric about the x_3 and x_1 axes, with the maximum displacement at the centre of the electrode, which coincides with the centre of the plate. The distribution is slightly elliptical because of the in-plane material anisotropy of quartz. We note that the vibration is mainly under the electrodes and decays rapidly outside them. This is the so-called energy trapping by the electrodes and the contour. The vibration decays to essentially zero near the plate edges where mounting can be designed without affecting the operation of the device. For this perfectly symmetric mode, it is known that the normal acceleration sensitivity of the resonator is zero,[19,20] which is ideal for frequency stability consideration of resonators when they are mounted on moving objects such as missiles and satellites.

When d is varied alone, the operating mode and its frequency are shown in Fig. 4 for three different values of d in increasing order. When d varies, the electrodes move up or down along x_3 in Fig. 2. Its effect is hardly noticeable in Fig. 4(a) when d is small. In Fig 4(b) it is visible that the vibration distribution has extended in the positive x_3 direction, following the shift of the electrodes. In a contoured resonator, both the electrodes and the contour affect energy trapping together. The vibration tends to be in the centre of the plate where the plate is thick, and also tends to be under the electrodes. In Fig. 4 the effect of the contour dominates. As the electrodes move up, the upper and lower boundaries of the vibrational region tend to follow the electrodes to some degree but the centre of the vibration is still trapped by the contour at the centre. In Fig. 4(c), the shift of the mode is very clear. We note that as d increases, the frequency increases. This is because as the electrodes move away from the plate centre where the vibration is large, the inertia of the electrodes is felt less and hence the frequency increases.

Figure 5 shows the corresponding case when b is varied alone and the electrodes move to the right in the positive x_1 direction. Similar to the behaviour in Fig. 4, as the electrodes shift to the right, the vibration distribution also extends to the right, but the centre of the vibration seems to be still roughly trapped at the plate centre, showing the dominance of the contour in this case. The frequency increases slightly from (a) to (c) as expected.

In Figure 6, both d and b are varied simultaneously while maintaining $b = d$. In this case, following the electrodes, the vibration distribution extends in the upper right direction as expected. The frequency also increases slightly.

To have a closer look at the effects of the electrode off centre on mode shapers, we plot the effect of d alone on mode shapes from Fig. 4 along $x_1 = 0$ in Fig. 7(a), and the effect of b alone on mode shapes from Fig. 5 along $x_3 = 0$ in Fig. 7(b). The loss of symmetry of the modes can be clearly seen in Fig. 7, which is important in resonator frequency stability consideration.[19,20] At present, the military requirement for the acceleration sensitivity of resonators on accelerating weapon systems is moving from $\frac{10^{-10}}{g}$ to $\frac{10^{-12}}{g}$ for the relative frequency shift per g. This is experiencing great challenges. The loss of mode symmetry contributes to acceleration sensitivity.[19,20] It is highly unde-

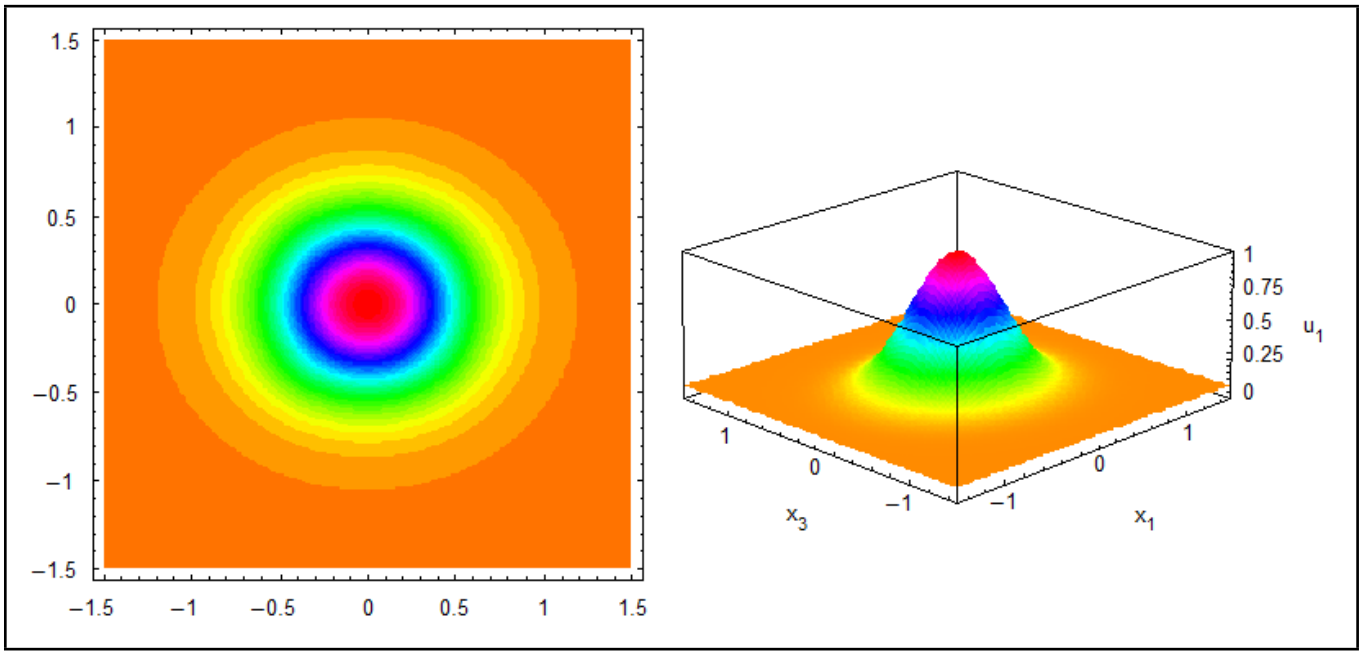

Figure 3. A perfect resonator without electrode off centre. $\omega_1 = 1.526029 \times 10^7 \frac{1}{s}$.

Table 1. Effect of electrode off centre on frequency.

Eccentric distance	$\omega_1(\times 10^7 \frac{1}{s})$	Relative difference (ppm)
$b = 0, d = 0.01a$	1.526030	0.7
$b = 0, d = 0.05a$	1.526035	4.0
$b = 0, d = 0.1a$	1.526053	15.7
$b = 0, d = 0.2a$	1.526128	64.9
$d = 0, b = 0.01a$	1.526030	0.7
$d = 0, b = 0.05a$	1.526036	4.6
$d = 0, b = 0.1a$	1.526057	18.3
$d = 0, b = 0.2a$	1.526141	73.4
$d = 0.01a, b = 0.01a$	1.526030	0.7
$d = 0.05a, b = 0.05a$	1.526042	8.5
$d = 0.1a, b = 0.1a$	1.526081	34.1
$d = 0.2a, b = 0.2a$	1.526238	136.9
$b = 0, d = 0$	1.526029	0.0

sirable and needs to be understood and controlled in resonator design and production.

In Fig. 8(a), $d = 0.2a$ is fixed while the radius of curvature R of the contour is increased to reduce the dominance of the contour. When R is large or the contour is less and hence the electrodes become more dominant in energy trapping, it can be seen that the loss of symmetry because of the electrode off centre becomes more prominent. Figure 8(b) shows the corresponding situation when $b = 0.2a$ is fixed and R is increased. The behaviour is similar to that in Fig. 8(a).

In Table 1, the relative frequency difference from a perfect resonator is shown for various values of electrode off centre. For the cases of $b = 0$ and $d = 0.01a$; $d = 0$ and $b = 0.01a$; and $d = b = 0.01a$ which have the smallest frequency difference, the relative frequency difference is of the order of one part per million (ppm). Most precision resonators are trimmed to frequency and an offset of 1 ppm due to electrode mis-registration is unimportant and is corrected for in the trimming process. However, the table shows that the frequency difference increases quickly as the electrode off centre becomes larger.

5. CONCLUSION

The trigonometric series used in the Ritz method converges rapidly and can produce frequencies with seven significant figures, accurate enough for ordinary resonator design. Numerical results show that when the energy trapping of the TSh vibration is dominated by the contour, the mode centre is still essentially at the plate centre but the distribution of the TSh vibration extends in the direction of the shift of the electrodes. Importantly, the TSh distribution loses its symmetry when there is an electrode off centre. This has important implications in resonator frequency stability consideration. In the typical resonator studied, when the electrode off centre is about one hundredth of the electrode length, the relative frequency shift is of the order of one part per million, not insignificant in resonator design and application.

ACKNOWLEDGEMENTS

This work was supported by the National Natural Science Foundation of China (No. 11272290). The last author was supported by Henan Province and Zhengzhou University through a Henan Provincial Visiting Professorship.

REFERENCES

[1] Zhang, T., Wang, Y., Liu, W. L., Cheng, J. G., Song, Z. T., Feng, S. L., Chan-Wong, L. H., and Choy, C. L. Fabrication and characterization of ZnO-based film bulk acoustic resonator with a high working frequency, Chin. Phys. Lett., **22** (3), 694–696, (2005). https://dx.doi.org/10.1088/0256-307X/22/3/048

[2] Wang, W. Y., Zhang, C., Zhang, Z. T., Liu, Y., and Feng, G. P. Lateral-field-excitation properties of LiNbO3 single crystal, Chin. Phys. B, **18** (2), 795–802, (2009). https://dx.doi.org/10.1088 /1056/18/2/064

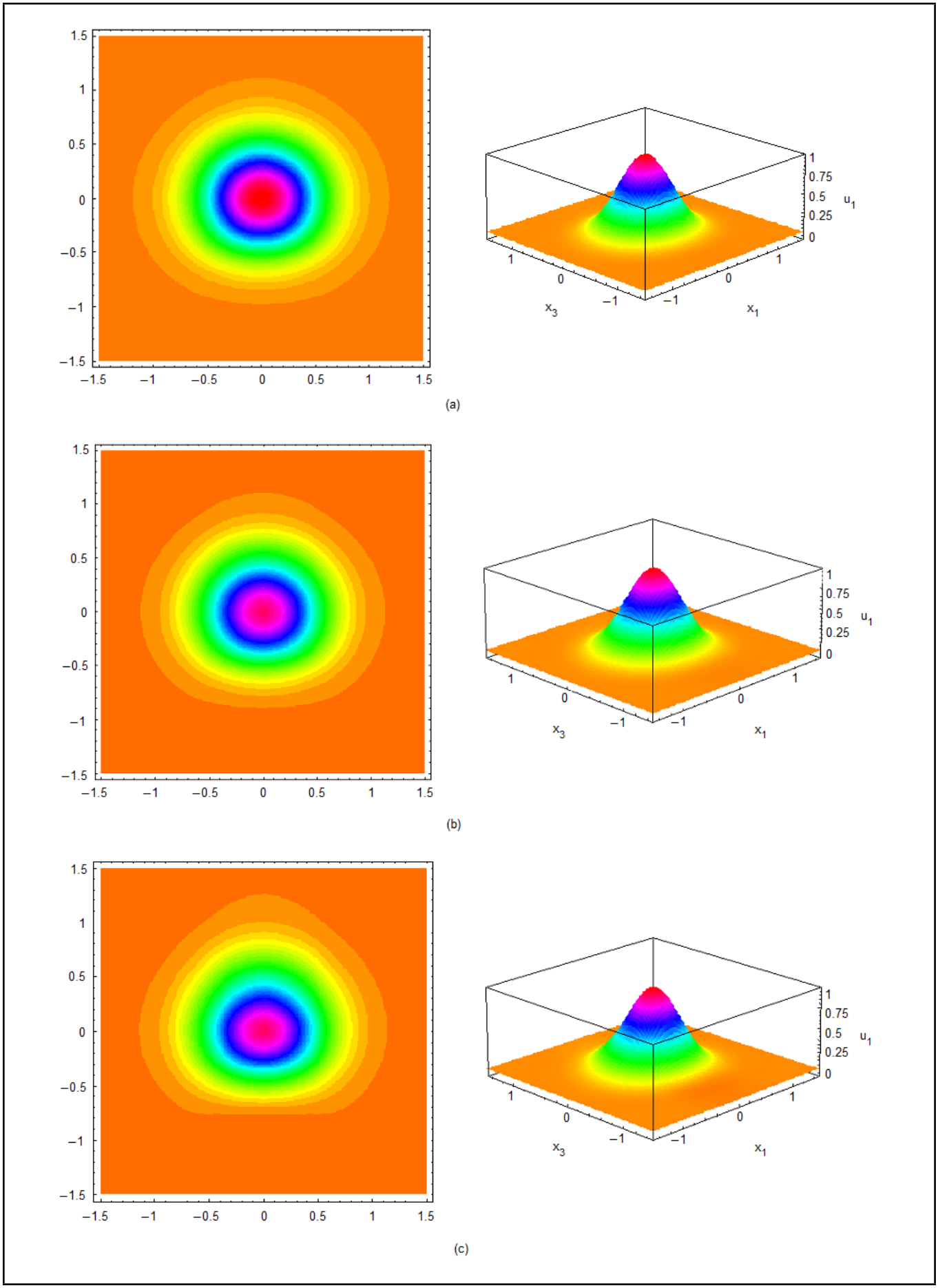

Figure 4. Effect of $d(b=0)$. (a) $d=0.1a, \omega_1=1.526053\times10^7 1/s$. (b) $d=0.2a, \omega_1=1.526128\times10^7 1/s$. (c) $d=0.5a, \omega_1=1.526693\times10^7 1/s$.

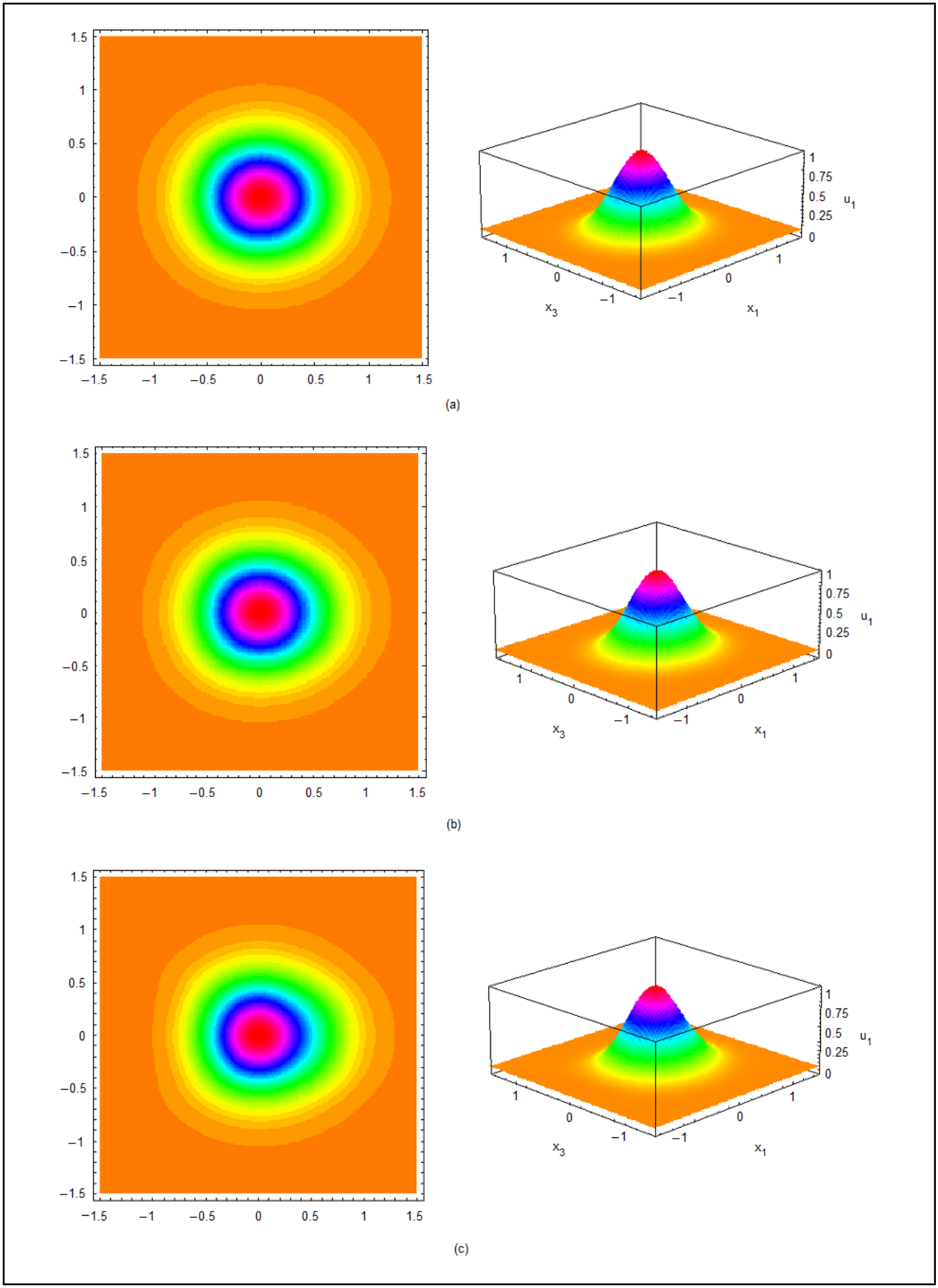

Figure 5. Effect of $b(d=0)$. (a) $b=0.1a, \omega_1 = 1.526057 \times 10^7 1/s$. (b) $b=0.2a, \omega_1 = 1.526141 \times 10^7 1/s$. (c) $b=0.5a, \omega_1 = 1.526746 \times 10^7 1/s$.

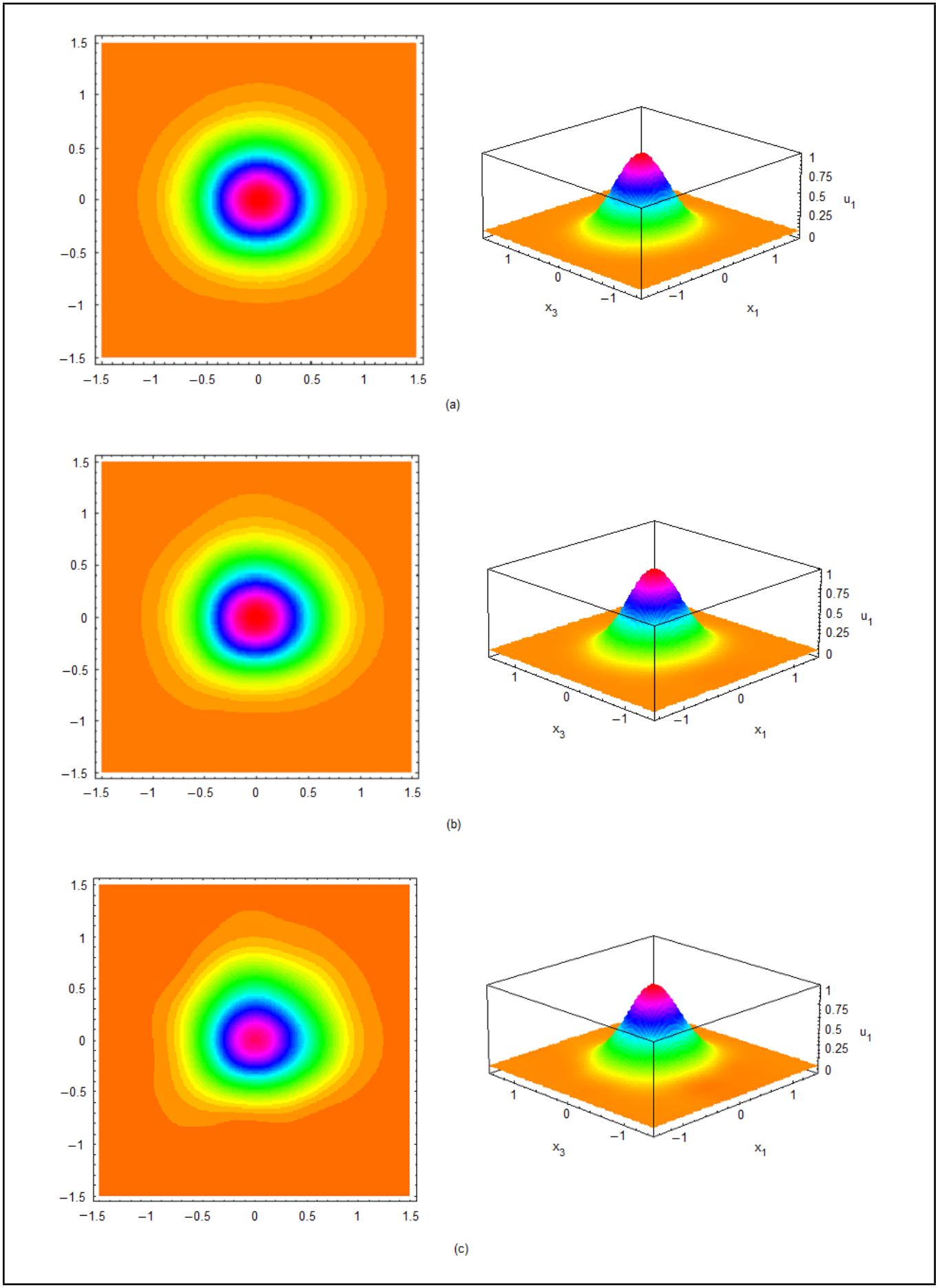

Figure 6. Both b and d are varying. (a) $d = b = 0.1a, \omega_1 = 1.526081 \times 10^7 1/s$. (b) $d = b = 0.2a, \omega_1 = 1.526238 \times 10^7 1/s$. (c) $d = b = 0.5a, \omega_1 = 1.527357 \times 10^7 1/s$.

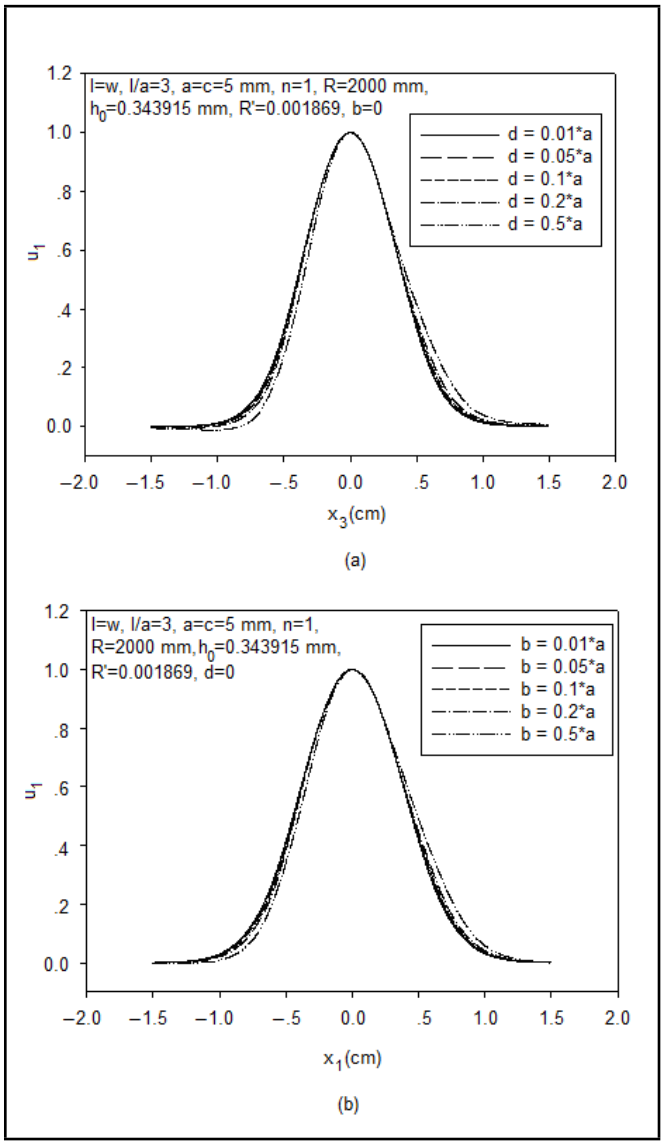

Figure 7. Effects of electrode off centre on mode shape. (a) Effect of d alone. (b) Effect of b alone.

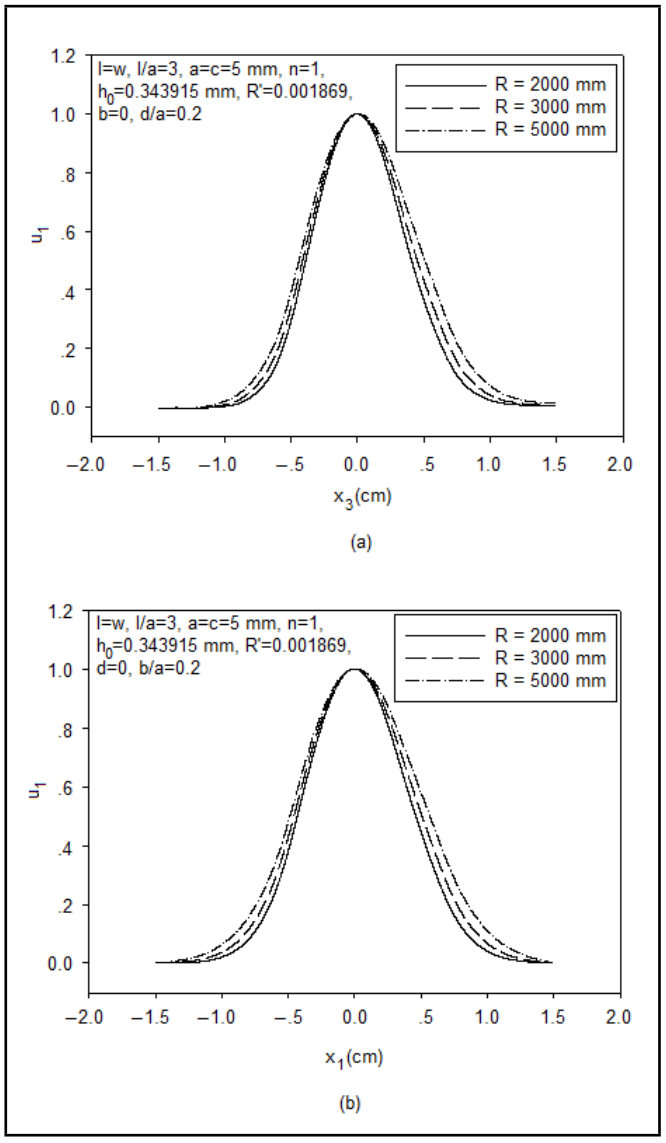

Figure 8. Effects of electrode off centre on mode shape for different values of R. (a) $b = 0, d = 0.2a$. (b) $d = 0, b = 0.2a$.

[3] Ma, T. F., Zhang, C., Feng, G. P., and Jiang, X. N. Lateral field excitation properties of langasite single crystal, Chin. Phys. B, **19** (8), 08770, (2010). https://dx.doi.org/10.1088/1674-1056/19/8/087701

[4] Ma, T. F., Zhang, C., Jian, X. N., and Feng, G. P. Thickness shear mode quartz crystal resonators with optimized elliptical electrodes, Chin. Phys. B, **20** (4), 047701, (2011). https://dx.doi.org/10.1088/1674-1056/20/4/047701

[5] Zhang, H. F., Turner, J. A., and Kosinski, J. A. Experimental measurements of the forcefrequency effect of thickness-mode langasite resonators, IEEE Trans. Ultrason., Ferroelect., Freq. Contr., **60** (7), 1475–1478, (2013). https://dx.doi.org/10.1109/TUFFC.2013.2719

[6] Xia, B. G., Zhang, H. D., Zhao, X., Yi, M., and Huang, J. Design and implementation of sub-reflector for Ka band antenna based on quartz wafer coating technology, Acta Phys. Sin., **62** (20), 204103, (2013). https://dx.doi.org/10.7498/aps.62.204103

[7] Liu, Y. Y., Dong, L., Wu, H. P., Zheng, H. D., Ma, W. G., Zhang, L., Yin, W. B., and Jia, S. T. All optical quartz-enhanced photoacoustic spectroscopy, Acta Phys. Sin., **62** (22), 220701, (2013). https://dx.doi.org/10.7498/aps.62.220701

[8] Gu, Y., Li, Q., Tian, F. F., and Xu, B. J. Structure and absorbability of a nanometer nonmetallic polymer thin film coating on quartz used in piezoelectric sensors, Chin. Phys. Lett., **30** (10), 108101, (2013). https://dx.doi.org/10.1088/0256-307X/30/10/108101

[9] Olsson, R. H., Hattar, K., Homeijer, S. J., Wiwic, M., Eichenfielda, M., Branchd, D. W., Bakera, M. S., Nguyena, J., Clarkb, B., Bauerc, T., and Friedmannca, T. A. A high electromechanical coupling coefficient SH0 Lamb wave lithiumniobate micromechanical resonator and a method for fabrication, Sensors and Actuators A-Physical, **209**, 183–190, (2014). https://dx.doi.org/10.1016/j.sna.2014.01.033

[10] Ko, W. and Jeon, S. An electrodeless quartz crystal resonator integrated with UV/Vis spectroscopy for the in-

vestigation of the photodecomposition of methylene blue, Sensors and Actuator-B Chemical, **193**, 774–777, (2014). https://dx.doi.org/10.1016/j.snb.2013.12.041

[11] Cao-Paz, A., Rodriguez-Pardo, L., and Farina, J. Temperature compensation of QCM sensors in liquid media, Sensors and Actuator-B Chemical, **193**, 78–81, (2014). https://dx.doi.org/10.1016/j.snb.2013.11.044

[12] Gu, Y., Li, Q., Xu, B. J., and Zhao, Z. Vibration analysis of a new polymer quartz piezoelectric crystal sensor for detecting characteristic materials of volatility liquid, Chin. Phys. B, **23** (1), 017804, (2014). https://dx.doi.org/10.1088/1674-1056/23/1/017804

[13] Gu, Y., and Li, Q. Application of the new pattern recognition system in the new e-nose to detecting Chinese spirits, Chin, Phys. B, **23** (4), 044213, (2014). https://dx.doi.org/10.1088/1674-1056/23/4/044213

[14] Boersma, F., and van Ballegooyen, E. C. Rotated Y-cut quartz crystal with two different electrodes treated as a one-dimensional acoustic composite resonator, J. Acoust. Soc. Am., **62** (2), 335–340, (1977). https://dx.doi.org/10.1121/1.381529

[15] Kosinski, J. A. Thickness vibrations of flat piezoelectric plates with massy electrodes of unequal thickness, Proc. IEEE Ultrasonics Symp., Honolulu, Hawaii, (2003). https://dx.doi.org/10.1109/ULTSYM.2003.1293358

[16] Wang, J. and Shen, L. J. Exact thickness-shear resonance frequency of electroded piezoelectric crystal plates, J. Zhejiang Univ. SCI, **6** (9), 980–985, (2005). https://dx.doi.org/10.1007/BF02857345

[17] Yang, J. S., Zhou, H. G., and Zhang, W. P. Thickness-shear vibration of rotated Y-cut quartz plates with relatively thick electrodes of unequal thickness, IEEE Trans. Ultrason., Ferroelect., Freq. Contr., **52** (5), 918–922, (2005). https://dx.doi.org/10.1109/TUFFC.2005.1503978

[18] He, H. J., Liu, J. X., and Yang, J. S. Effects of Mismatched Electrodes on an AT-cut Quartz Resonator, IEEE Trans. Ultrason., Ferroelect., Freq. Contr., **59**, 281–286, (2011). https://dx.doi.org/10.1109/TUFFC.2012.2188

[19] Zhou, Y. S., and Tiersten, H. F. On the normal acceleration sensitivity of contoured quartz resonators with the mode shape displaced with respect to rectangular supports, J. Appl. Phys., **69** (5), 2862–2870, (1991). https://dx.doi.org/10.1063/1.348594

[20] Kosinski, J. A., and Pastore, R. A. Theory and design of piezoelectric resonators immune to acceleration present state of the art , IEEE Trans. Ultrason., Ferroelect., Freq. Contr., **48** (5), 1426–1437, (2001). https://dx.doi.org/10.1109/58.949753

[21] Tiersten, H. F., Lwo, B. J., and Dulmet, B. Transversely varying thickness modes in trapped energy resonators with shallow and beveled contours, J. Appl. Phys., **80** (2), 1037–1046, (1996). https://dx.doi.org/10.1063/1.362838

[22] Tiersten, H. F. Analysis of intermodulation in thickness-shear and trapped energy resonators, J. Acoust. Soc. Am., **57** (3), 667–681, (1975). https://dx.doi.org/10.1121/1.380491

[23] Tiersten, H. F. Analysis of trapped-energy resonators operating in overtones of coupled thickness-shear and thickness-twist, J. Acoust. Soc. Am., **59** (4), 879–888, (1976). https://dx.doi.org/10.1121/1.380947

[24] Tiersten, H. F., and Smythe, R. C. An analysis of contoured crystal resonators operating in overtones of coupled thickness shear and thickness twist, J. Acoust. Soc. of Am., **65** (6), 1455–1460, (1979). https://dx.doi.org/10.1121/1.382907

[25] Tiersten, H. F., and Smythe, R. C. Coupled thickness-shear and thickness-twist vibrations of unelectroded AT-cut quartz plates, J. Acoust. Soc. of Am., **78** (5), 1684–1689, (1985). https://dx.doi.org/10.1121/1.392754

[26] Stevens, D. S., and Tiersten, H. F. An analysis of doubly rotated quartz resonators utilizing essentially thickness modes with transverse variation, J. Acoust. Soc. Am., **79** (6), 1811–1826, (1986). https://dx.doi.org/10.1121/1.393190

[27] Shi, J. J., Fan, C. Y., Zhao, M. H., and Yang, J. S. Variational formulation of the Stevens-Tiersten equation and application in the analysis of rectangular trapped-energy quartz resonators, J. Acoust. Soc. Am., **135** (1), 175–181, (2014). https://dx.doi.org/10.1121/1.4829535

[28] Shi, J. J., Fan, C. Y., Zhao, M. H., and Yang, J. S. Trapped thickness-shear modes in a contoured, partially electroded AT-cut quartz resonator, Eur. Phys. J-Appl. Phys., **69** (1), 10302.1–10302.7, (2015). https://dx.doi.org/10.1051/epjap/2014140278